Biosensors and Bioelectronics 117 (2018) 480–486

Contents lists available at ScienceDirect

Biosensors and Bioelectronics

journal homepage: www.elsevier.com/locate/bios

Magnetic force assisted electrochemical sensor for the detection of thrombin with aptamer-antibody sandwich formation

Saeromi Chung[a], Jong-Min Moon[a], Jaekyu Choi[b], Hyundoo Hwang[b,*], Yoon-Bo Shim[a,*]

[a] Department of Chemistry, Pusan National University, 2 Busandaehak-ro 63beon-gil, Geumjeong-gu, Busan 46241, Republic of Korea
[b] BBB Inc., 26 Samseong-ro 85-gil, Gangnam-gu, Seoul 06194, Republic of Korea

ARTICLE INFO

Keywords:
Thrombin
Electrochemistry
Aptamer
Sandwich assay
Magnetic force

ABSTRACT

A magnetic force assisted electrochemical aptamer-antibody sandwich assay (MESA) was developed for the detection of thrombin as a model protein in serum samples. The MESA using the formation of sandwich complexes on the electrochemical sensor probe for reaction and the removal of unbound bioconjugates from the sensor surface without washing are controlled by a magnetic field. Thrombin was determined by the cathodic currents of a toluidine blue O (TBO) attached with thrombin antibody modified magnetic nanoparticle (MNP) at the sensor surface. To detect thrombin in a serum sample, we applied a thrombin-specific aptamer as the capture molecule bound to the functionalized conducting polymer layer (poly-(2,2′:5′,5″-terthiophene-3′-p-benzoic acid) (pTBA)), and streptavidin and starch coated-MNP was conjugated with biotinylated thrombin antibodies (Ab) and TBO as the bioconjugate (MNP@Ab-TBO). The characterization of MNP@Ab-TBO and sensor probe was performed using voltammetry, impedance spectroscopy, XPS, and UV–VIS spectroscopy. The experimental conditions were optimized in terms of pH, binding time, removal time of unbound bioconjugates, and applied potential. The dynamic ranges of thrombin were from 1.0 to 500 nM with detection limit of 0.49 (± 0.06) nM. The recovery test demonstrates the reliability of the proposed sensing system for a handheld device.

1. Introduction

Thrombin is a serine protease, which plays an important role in the blood coagulation cascade. It catalyzes many coagulation-related reactions including the conversion of fibrinogen to insoluble fibrin (Tasset et al., 1997). The coagulation protease thrombin also regulates critical cellular responses in hemostasis and thrombosis, inflammation, and blood vessel development (Coughlin, 2000). Besides, evidences have been reported to support the hypothesis that thrombin serves to activate tumor growth, metastasis, and angiogenesis (Inuyama et al., 1997; Nierodzik and Karpatkin, 2006). Therefore, it is reasonable to say that thrombin in blood is a relevant marker to estimate some diseases including thrombosis, vascular injuries, and metastatic cancers. Hence, various assay methods including clotting assays (Macfarlane and Biggs, 1953), surface enhanced Raman spectroscopy (Gao et al., 2015a), enzymatic activity assays (Luddington and Baglin, 2004), and immunoassays (Shuman and Majerus, 1976; Rand et al., 1996) have been applied to quantitatively detect thrombin in the blood. Although these methods can provide good performance, they suffer from somewhat drawbacks, such as long analysis time, requiring specialists, and high cost, which make them less suitable for hand-held device applications. Thus, a simple and robust protein detection method is needed. One of candidates is electrochemical sensors using aptamers (Willner and Zayats, 2007; Min et al., 2010) as an alternative thrombin analysis method. This can offer clear advantages of the possibility to miniaturize a detection system with high sensitivity, low cost, independence from sample volume, and less interferences in real samples (Chandra et al., 2012). Hence, there have been much efforts to develop robust electrochemical sensors for the thrombin detection (Gao et al., 2015b, 2016; Qian et al., 2015; Wang et al., 2017).

For the last two decades, aptamers have attracted much attention of researchers in biosensor applications, due to their remarkable features in terms of high specificity and affinity to a wide range of molecular targets, ease of synthesis, high stability, flexibility in labeling at a desired site without loss of activity, and weak immunogenicity (Iqbal et al., 2000; Tan et al., 2004). One of them, thrombin aptamers have been extensively sought and the most widely used to demonstrate the proof-of-concept of the aptamer-based assays or sensors. To do this, aptamers could be immobilized using supporting materials, such as conducting polymers (Moon et al., 2018), gold-thiol interactions (Min et al., 2010), hydrogel particles (Srinivas et al., 2011) or magnetic beads (Tennico et al., 2010), to capture target molecules in sample

* Corresponding authors.
E-mail addresses: doo@bbbtech.com (H. Hwang), ybshim@pusan.ac.kr (Y.-B. Shim).

https://doi.org/10.1016/j.bios.2018.06.068
Received 14 May 2018; Received in revised form 28 June 2018; Accepted 29 June 2018

solutions. Of these, conducting polymers having functional group of carboxylic acid or amine are rather excellent substrate than the others to immobilize biomaterial and catalysts on the sensor probe, which have electrically conductive and biologically compatible properties (Koh et al., 2011). Thus, to enhance the sensor performance along with stability and sensitivity, using a functionalized conducting polymer is one of the finest methods to bind biomaterial through the covalent bond formation (Naveen et al., 2017).

Among the electrochemical aptasensor, the sandwich assay format has still been widely applied for the detection of proteins. In case of the target protein having two binding sites for two distinct aptamers, the target can be captured by binding to the capture aptamer on the electrode, and then form a sandwich complex with the second aptamer conjugated with a redox indicator (horseradish peroxidase (Mir et al., 2006), platinum nanoparticles (Polsky et al., 2006), and toluidine blue O (Moon et al., 2017)), which generates electrochemical response. However, it has been reported that only few kinds of proteins have two aptamer binding sites, thus most of the sandwich protein assays have focused on conventional antibody-based immunoassays or assays based on aptamer-antibody pair (He et al., 2007; Zhu et al., 2013). Moreover, the sandwich protein assays still face challenges that they necessarily require time- and reagent-consuming washing and repetitive steps, regardless of the detection methods. For the last decade, the miniaturized point-of-care devices have been studied to provide the advantages of portability and automation using fluorescence sandwich immunoassay (Fan et al., 2008), and ELISA (Chin et al., 2011). However, those devices still require pre-stored buffers and reagents for washing and reaction, as well as external pumping elements to transfer the sample and reagents inside the device. To solve this limitation, a few attempts have been made to eliminate pumping and buffer exchange steps in the sandwich protein assay protocols using electrokinetic mechanisms (Hwang et al., 2010). Nevertheless, this method also has a limitation which efficiency is sensitive to the electrical properties of samples.

To overcome the disadvantage using extra washing step of immunoassay, we introduce a methodology called magnetic force-assisted electrochemical sandwich assay (MESA), where the formation of sandwich complexes on electrochemical sensor probe for reaction and the removal of unbound bioconjugates from the sensor surface are controlled by a magnetic field, and the amount of analyte is quantified by measuring the electrochemical signals from the bioconjugates bound onto the sensor surface. In particular, the electrochemical sandwich assay combined with the magnetic beads have been developed as a purpose of electrode probe (Centi et al., 2007; Eguílaz et al., 2010; Han et al., 2016). However, there were no report using bioconjugated magnetic bead as an electrochemical label to minimize the reaction/washing step, to date.

In this study, to detect thrombin from a serum sample, we applied thrombin-specific aptamer as the capture molecule bound to the functionalized conducting polymer layer (poly-(2,2′:5′,5″-terthiophene-3′-p-benzoic acid) (pTBA)), and streptavidin-starch modified magnetic nanoparticle (MNP) combined with toluidine blue O (TBO) and biotinylated thrombin antibodies (Ab) as the bioconjugates. The MESA enables to quantify the amount of target analytes in a tiny amount of sample droplet without any moving elements or buffer exchange steps as well as without any bulky and expensive detection components. This method would provide a solution for the needs of point-of-care testing market, which have sought a method for simple, automated, rapid, and accurate detection of disease markers from a drop of biological fluids using a handheld device.

2. Experimental

2.1. Materials

Di(propylene glycol) methyl ether, tri(propylene glycol) methyl ether, 1,1′-carbonyldiimidazole (CDI), toluidine blue O (TBO), thrombin, 1-(3-dimethylaminopropyl) −3- ethylcarbodiimide (EDC), N-hydroxysuccinimide (NHS) were purchased from Sigma-Aldrich (St. Louis, MO, USA). 100 nm size starch-coated bionized nanoferrite particles with streptavidin on surface (MNP) was purchased from Micromod Partikeltechnologie GmbH (Rostock, Germany). Biotin-conjugated human thrombin antibody was purchased from Abcam (Cambridge, UK). The amine terminated thrombin aptamers were obtained from Bioneer Co. (South Korea), which have the following sequences: 5′GGT TGG TGT GGT TGG-C_6 3′amine. Prior to using the aptamer, a stock solution was prepared as follows: the aptamer was denatured for 3 min at 95 °C, incubated for 1 h at 4 °C. A terthiophene monomer bearing a benzoic acid group, 2,2′:5′,5″-terthiophene-3′-p-benzoic acid (TBA) was synthesized according to a previous report (Kim et al., 2012). Phosphate buffered saline (PBS) solutions were prepared with 0.1 M disodium hydrogen phosphate (Sigma-Aldrich), 0.1 M sodium dihydrogen phosphate (Sigma-Aldrich). All the aqueous solutions were prepared in doubly distilled water, which was obtained from a Milli-Q water-purification system (18 MΩ cm).

2.2. Instruments

The screen-printed carbon electrodes (SPCEs) were composed of carbon, Ag/AgCl, and carbon as the working, reference, and counter electrodes, respectively. Carbon and silver inks (Jujo Chemical, Japan) were printed on the polystyrene-based film using a screen printer (BANDO Industrial, Korea). Cyclic voltammogram and chronoamperogram were recorded using a potentiostat (Kosentech Model PT-1). The electrochemical impedance spectra (EIS) were measured with an EG & G Princeton Applied Research PARSTAT 2263 at an open-circuit voltage from 100 kHz down to 100 mHz, at a sampling rate of five points per decade (AC amplitude: 10 mV). The electric-magnet was obtained by BBB incorporation (South Korea). The electric-magnet was operated by Laboratory DC power supply gps 3303 (12 V). The morphology of MNP@Ab-TBO particles was characterized by transmission electron microscopy (TEM; TALOS F200X) and UV–Vis spectrometer (UV-1800).

2.3. Preparation of magnetic nanoparticle conjugate

At first, 5 mL of streptavidin-starch coated magnetic nanoparticles (0.5 mg/mL in 0.02% sodium azide) (MNPs) was incubated with the 0.5 mL of 150 μg/mL biotinylated anti-thrombin antibody for 1 h at room temperature. Thereafter, the MNPs conjugated with antibodies were collected with a permanent magnet, followed by washing with 0.1 M PBS solution. The collected MNPs were incubated in 5 mL of 20 mM CDI in 0.1 M PBS for 6 h at 8 °C. The MNPs were collected by a permanent magnet, then reacted in 5 mM TBO in 0.1 M PBS solution overnight at 8 °C. The MNPs@Ab coated with TBO (MNPs@Ab-TBO) were collected and washed using a permanent magnet.

2.4. Fabrication sensor probes

The screen-printed carbon electrodes (SPCEs) were manufactured on the polyethylene-based film using a screen printer (BANDO industrial, Korea). Silver was coated on the film as conductor, and then carbon was printed as working and counter electrodes. Then insulator was also covered on the top of the film. To modify the surface of the working electrode, 1 mM TBA in a 1:1 mixture of dipropylene glycol methyl ether and tripropylene glycol methyl ether was dropped onto the working electrode, then dried at 60 °C for 1 h in the dry oven. The monomers were electrically polymerized via CV with potential cycling from 0.0 V to 1.2 V (vs. Ag/AgCl) for 2 cycles at 0.1 V/s in 0.1 M PBS (pH 7.4). The amine terminated thrombin aptamer (2 μM) was immobilized on the benzoic acid functionalized conducting polymer layer (poly-TBA) with EDC/NHS coupling. Each modification step was verified using CV and EIS. The sensor chamber was fabricated using the screen-printed electrode, polyethylene cover (thickness: 1.2 mm), and

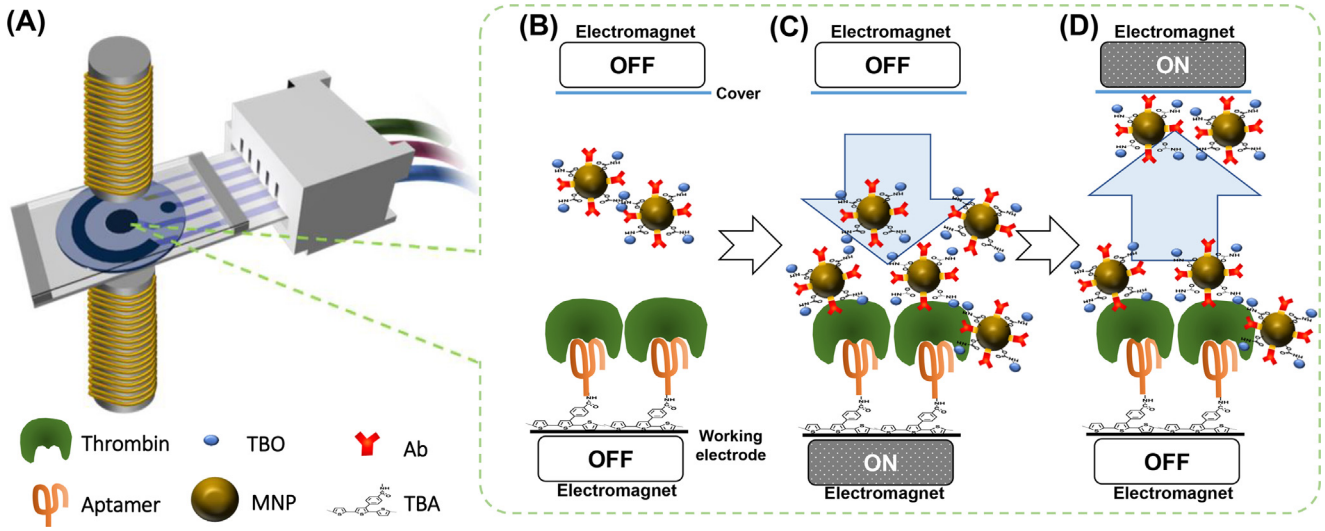

Scheme 1. (A) The system is composed of an electrochemical sensor, a pair of electromagnets, and a sample chamber. (B-D) The process of MESA is illustrated: (B) the sample loading step to mix the sample solution and the magnetic nanoparticle bioconjugates (MNP@Ab-TBO); (C) the reaction step to form sandwich complexes on the electrode surface; and (D) the removal step to remove unbound MNP@Ab-TBO from the electrode surface.

acryl glue coated polyethylene/acryl walls.

3. Results and discussion

A schematic diagram and the principles of the aptamer-antibody based magnetic force-assisted electrochemical sandwich assays (MESA) are as shown in Scheme 1. The system is composed of electrodes, a pair of electromagnets for controlling the magnetic fields, and a sample chamber (Scheme 1 (a)). Once the sample solution containing analytes (thrombin) arrives at the chamber, the sample is mixed with the MNPs conjugated with the electrochemical redox label (TBO) and the secondary capture molecules (thrombin antibody) specifically bind to the analyte (Scheme 1 (b)). The primary capture molecules (thrombin-specific aptamers) are immobilized on the working electrode, which locates in the sample chamber. In this study, a conducting polymer, pTBA having carboxylic acid group, was applied to immobilize the amine modified aptamer on the working electrode of screen-printed carbon electrode (SPCE). The TBO and antibody modified MNP conjugate (MNP@Ab-TBO) bound to the analytes, and it can form “sandwich" complexes with the capture molecules (aptamer) on the surface of working electrodes. The process forming sandwich complexes on the electrode surface can be facilitated by the application of a magnetic field driving MNP bioconjugates toward the working electrode (Scheme 1 (c)). To quantify the amount of analyte in the sample solution, the amount of MNP@Ab-TBO formed sandwich complexes on the electrode surface should be analyzed via electrochemical measurements. Before measuring the signal, however, the process for removing unbound probes is necessarily required to obtain reliable quantitative data with a minimal background signal. Instead of washing out with buffer solution, in this method, the electromagnet locates on the other side of the sample chamber is turned on, while the one on the electrode-side is turned off, to pull the unbound MNPs far from the working electrode (Scheme 1 (d)). As consequences, one can measure the electrochemical signals only from the MNP@Ab-TBO bound onto the working electrode by forming sandwich complexes, enabling to quantify the amount of analyte from a small amount of liquid sample with neither any moving parts nor heavy, expensive, complicated detection system.

3.1. Characterization of electrochemically-labeled magnetic nanoparticle (MNP) bioconjugates

To demonstrate the MESA for the detection of thrombin, first of all, the MNP conjugate coated with electrochemical redox labels and thrombin antibody were prepared. The starch coated MNPs with streptavidin on the surface were incubated with biotinylated thrombin antibody (Ab) to immobilize the Ab on the particle surface by the streptavidin-biotin interaction. The hydroxyl groups of the MNP surface were activated by 1,1′-carbonyldiimidazole (CDI) treatment, followed by incubation with a TBO solution to immobilize TBO, as the electrochemical redox label.

The transmission electron microscopic image of the MNP bioconjugates with TBO and Ab (MNP@Ab-TBO) shows that there was no aggregation or structural changes after the surface modification processes (Fig. 1(A)). The treated MNPs still showed high mobility under a magnetic field generated by a permanent magnet (Fig. 1(B)), which means that they are stable enough to be a relevant detection material for the MESA, where the magnetic mobility and stability of the bioconjugates are the most important factors for rapid and reproducible sandwich assays based on the magnetic force. In the UV–Vis spectra shown in Fig. 1(C), two characteristic absorption peaks of TBO at around 288 and 633 nm, and one absorption peak of TBO dimer at around 598 nm (Jebaramya et al., 2009) are clearly shown in the spectrum of TBO. The absorbance spectrum of streptavidin-coated MNPs is also consistent with the results from previous literatures, where the absorbance of bare iron oxide particles steadily decreased from 200 to 800 nm (Gong et al., 2007) and red fluorescence labeled-streptavidin has a peak at around 280 nm (Green, 1970). The spectrum of the MNP@Ab-TBO showed the characteristics of both materials, iron oxide and TBO, meaning that the MNPs contains TBO, which can be used as an electrochemical redox label. The electrochemical properties of the MNP@Ab-TBO were also characterized using cyclic voltammetry (CV). The MNP@Ab-TBO were suspended in 0.1 M PBS solution and the CV curve was recorded in potential range −150 mV to −450 mV as shown in Fig. 1(D). We could find clear redox peaks between −275 mV and −325 mV in the presence of MNP@Ab-TBO. These results indicate that the MNP@Ab-TBO that we have prepared are relevant materials for the quantitative detection of thrombin based on the MESA.

3.2. Characterization of aptamer-antibody sandwich complex formation

Electrochemical impedance spectroscopy (EIS) was employed to verify each process for the fabrication of aptamer-based sensors and the aptamer-antibody based sandwich assays. For the preparation of sensing electrodes, the working electrode surface was coated with pTBA

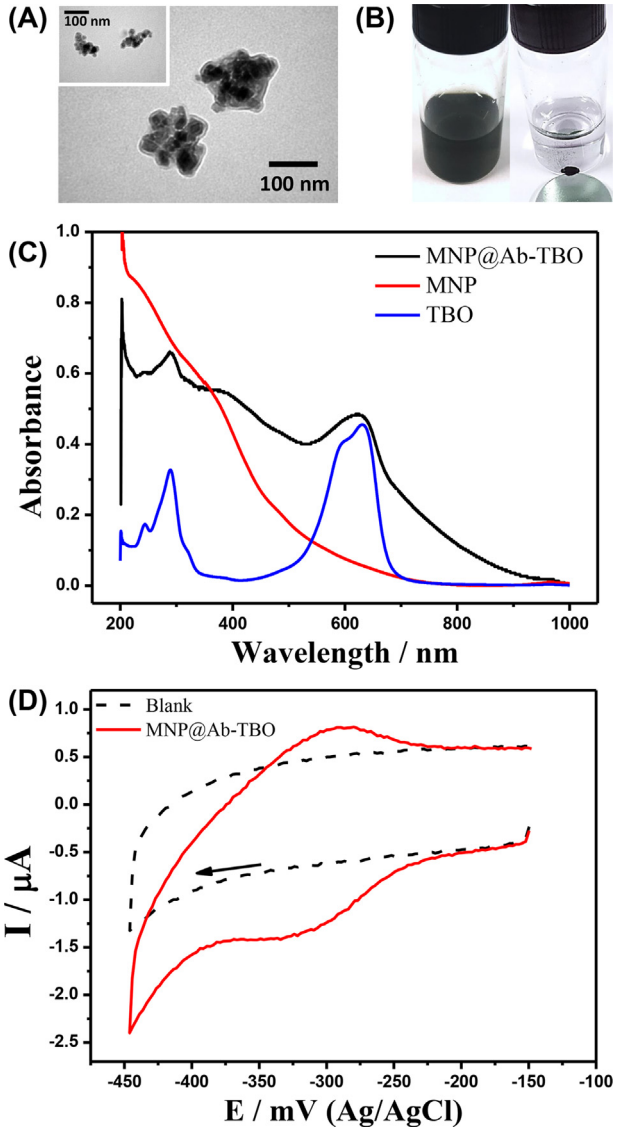

Fig. 1. (A) The TEM images of the MNP@Ab-TBO (Inset: the TEM image of MNP particles), (B) The image of MNP@Ab-TBO solution with and without the particles collection on the magnet, (C) UV–Vis. spectra obtained for bare MNPs, TBO, and MNP@Ab-TBO, and (D) CVs of MNP@Ab-TBO (solid line) with magnetic force, and blank (dashed line) in 0.1 M PBS solution.

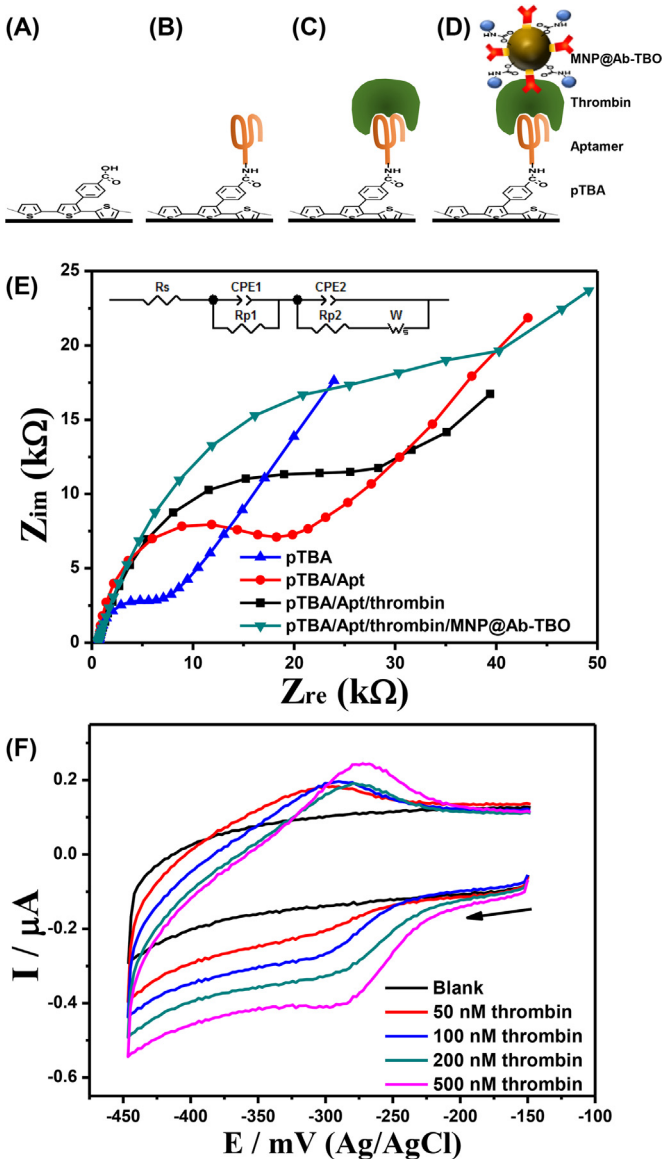

Fig. 2. Illustrations showing the processes of sandwich complex formation: (A) modification of carbon electrodes with a conducting polymer, pTBA; (B) immobilization of thrombin-specific aptamers; (C) recognition of thrombin; and (D) binding of MNP@Ab-TBO. (E) Nyquist plots for pTBA, pTBA/Apt, pTBA/Apt/thrombin, and pTBA/Apt/thrombin/MNP@Ab-TBO in 0.1 M PBS (pH 7.4). (F) CVs of different concentrations of thrombin from 0 to 500 nM in 0.1 M PBS (pH 7.4) using the electrochemical aptamer-antibody sandwich assay.

(Fig. 2(A)), then thrombin-specific aptamers were immobilized on the electrode (Fig. 2(B)). During the sandwich immunoassays, thrombin molecules were recognized by the aptamers (Fig. 2(C)), followed by binding of MNP@Ab-TBO on the surface (Fig. 2(D)). At each step, the charge transfer resistance (R_{ct}) was measured using the Nyquist plots of electrodes in the presence of 3 mM $[Fe(CN)_6]^{3-/4-}$ in KNO_3 as shown in Fig. 2(E). The R_{ct} was 8.08 kΩ just after the polymerization of TBA on the SPCE. The R_{ct} increased gradually to 21.5 kΩ, 34.74 kΩ, and 52.89 kΩ after the immobilization of aptamers, the recognition of thrombin, and the binding of MNP@Ab-TBO, respectively. The reason is that the biomolecules interfere with the charge transfer and hinder the access of redox material to the electrode surface.

To confirm the functionality of this assay with different amount of analyte, CV at different concentrations of thrombin from 0 to 500 nM were measured as shown in Fig. 2(F). Here the final removal step was done by applying a magnetic field to remove the unbound MNP@Ab-TBO. As the concentration of thrombin increased, the reduction peak significantly increased. These results indicate that the immobilization of aptamers and the binding processes of the aptamer-antibody based sandwich assays are functioning properly, and the aptamer-antibody sandwich assay based on the direct detection of redox materials can be applied for quantitative detection of protein markers.

To characterize the modification of the sensing probes, the deconvoluted XPS spectra of S2p, C1s, N1s, P2p, and Fe2p were investigated as shown in Fig. 3. The S2p spectrum showed two peaks at 164.80 and 163.59 eV, indicating C=S, and C-S, respectively because of the terthiophene backbone of pTBA (Fig. 3(A)). As shown in Fig. 3(B), the C1s peaks of pTBA layer appeared at 286.54 (COOH), 284.97 (sp^3C), and 284.46 eV (sp^2C). After modification of aptamer (pTBA/Apt), the N-C=O peak corresponding to the covalent bonding between pTBA and aptamer and the C=O peak of aptamer component newly appeared at 286.60 and 285.57 eV, respectively. In addition, the COOH peak was slightly shifted to higher energy at 287.74 eV. The pTBA/Apt/thrombin layer showed C1s peaks corresponding of COOH, N-C=O, and C=O bonds at 287.90, 288.44, and 285.59 eV, where they shifted to high

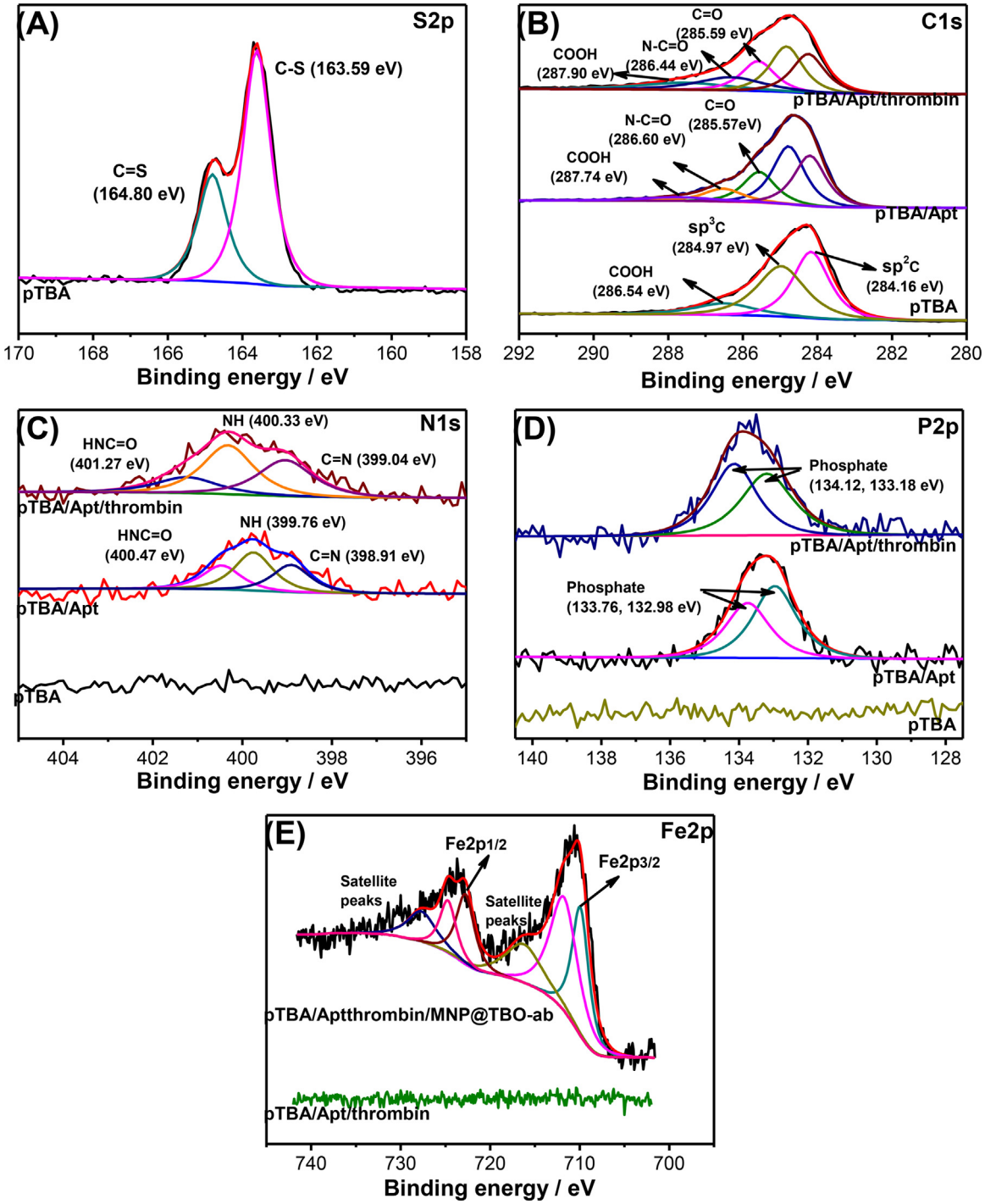

Fig. 3. (A) XPS spectra of modified senor probe of the (A) S2p, (B) C1s, (C) N1s, (E) P2p, and (E) Fe2p peaks for the pTBA, pTBA/Apt, pTBA/Apt/thrombin, and pTBA/Apt/thrombin/MNP@Ab-TBO.

energy than that of pTBA/Apt due to the thrombin captured by aptamer layer. The N1s spectrum for pTBA/Apt layer exhibited three new peaks at 400.47 (HNC=O), 399.76 (N-H), and 398.91 eV (C=N) (Fig. 3(C)). This result indicated that the covalent bond was formed between the COOH of pTBA and the NH_2 of aptamer. After thrombin interaction with the aptamer (pTBA/Apt/thrombin), the all N1s peaks shifted to the high energy at 401.27, 400.33, 399.04 eV, respectively, compared to the pTBA/Apt layer. Moreover, the P2p spectrum of pTBA showed no peak, while pTBA/aptamer layer showed the phosphate peaks at 133.76, and 132.98 eV due to aptamer molecules (Fig. 3(D)). Finally, the pTBA/Apt/thrombin/MNP@Ab-TBO layer was confirmed by the Fe2p spectrum, where showed clear peaks of $Fe2p_{1/2}$ and $Fe2p_{3/2}$, and satellite peaks due to the presence of MNP bioconjugates (Fig. 3(E)). However, no peaks of Fe2p were observed at pTBA, pTBA/Apt, and pTBA/Apt/thrombin surface. These results indicated that the successful modifications were carried out.

3.3. Optimization of analytical parameters

To find an optimal condition for the thrombin detection using MESA, the change in the amperometric current was measured by varying the pH, thrombin binding time, MNP@Ab-TBO binding time,

removal time of unbound bioconjugates, and applied potential. As shown in Fig. S1(A), the effect of pH was examined in the range of pH 6.5–8.5. The maximum response was observed at pH 7.4, and this pH was selected as optimal condition. The thrombin binding time to pTBA/Apt was optimized from 0 to 8 min (Fig. S1(B)). The peak current increased to the 3 min and reached steady state. The binding time of MNP@Ab-TBO to the pTBA/Apt/thrombin was optimized from 0.2 to 10 min as shown in Fig. S1(C). The response was gradually increased to the 4 min, then reached steady state. This might be due to the saturation of thrombin/MNP@Ab-TBO to the aptamer. Thus, the optimized binding time was determined to be 4 min. The removal time of non-binding thrombin/MNP@Ab-TBO by applying the magnetic field from the opposite side to the aptasensor was examined from 2 to 15 s (Fig. S1(D)). The response current was gradually decreased from 2 to 10 s, and then it reached steady state at 10 s. Therefore, removal time was chosen at 10 s. Finally, the applied potential for thrombin detection was studied between −275 to −400 mV (Fig. S1(E)). The response current was increased from −275 to −350 mV, and it decreased at potentials less than −350 mV. The maximum current was determined at −350 mV which was used for the subsequent experiments. Additionally, control experiments were examined to evaluate the adsorption of thrombin/MNP@Ab-TBO on the pTBA modified sensor probe in PBS saline (pH 7.4). As shown in Fig. S2(A), cyclic voltammetric response was not observed after removal step using a magnet or PBS buffer solution. On the other hand, when the 200 nM of thrombin/MNP@Ab-TBO was applied to aptasensor, both magnetically- and PBS-washed sensors revealed the cyclic voltammetric response of TBO (Fig. S2(B)). From this, the proposed aptasensor revealed a good selectivity toward thrombin without non-specific binding in human serum sample. Thus, it can be applied for further thrombin analysis. The reproducibility of the present method was evaluated using five different sensors, which showed a relative standard deviation of < 4.3% at a thrombin concentration of 200 nM. The long-term stability was evaluated every two or three days using 200 nM thrombin. The response of sensors retained more than 94% of their initial response for 24 days at room temperature

3.4. Amperometric sensor for thrombin based on MESA

The proposed sensor was monitored by amperometry under optimized conditions. Each thrombin solution (25 μL) was loaded to the pTBA/Apt chamber. After 3 min of thrombin binding time, MNP@Ab-TBO solution (25 μL) was injected to the chamber and incubated with magnetic force. After 4 min, unbound MNP@Ab-TBO was washed using magnet for 10 s. Then, the reduction current of TBO was measured. Fig. 4 shows the amperometric response of sensor and calibration plot of thrombin. The linear regression equation of the calibration plot showed the ΔI_P (nA) = 4.022 (± 0.481) + 0.208 (± 0.007) [thrombin] (nM) with correlation coefficiency of 0.991. The current response of TBO in the MNP shows linear range from 1 to 500 nM. The detection limit of thrombin was 0.49 (± 0.06) nM using ten blank noise signals (95% confidence level, $k = 3$, $n = 10$). Through this experiment, we found that the magnetic force could selectively remove the unbound MNP@Ab-TBO, while the MNP@Ab-TBO formed sandwich complexes with aptamer-antibody pairs remained on the surface of working electrode, enabling the quantitative detection of thrombin based on the MESA in a reliable manner. The MESA enables to exclude the washing reagents and fluidic handling, which have been one of main challenges that most of conventional heterogeneous assays had to overcome for miniaturization. A Table S1 shows the analytical performance of various analytical methods for thrombin detection.

3.5. Real sample analysis

The detection of thrombin relies on the affinity reaction between pTBA/Apt/thrombin and MNP@Ab-TBO. The complexation of

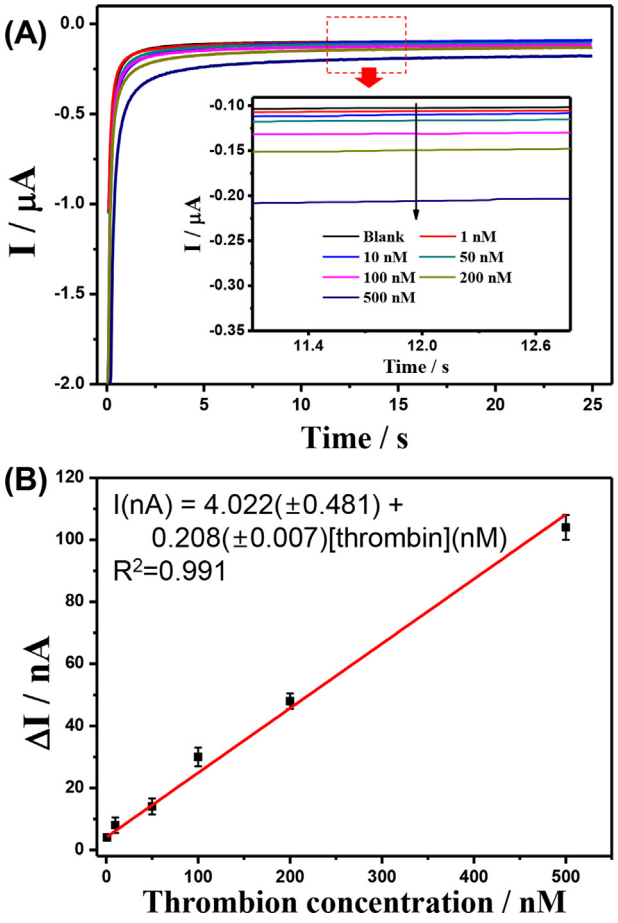

Fig. 4. (A) The amperometric responses for various concentrations of thrombin using MESA assay in 0.1 M PBS, applied potential: −350 mV (inset: magnified chronoamperometric signal from 11 to 12.8 s) (B) Calibration plot based on the signals obtained in the chronoamperometric responses.

MNP@Ab-TBO with thrombin allows the detection of thrombin by the electrochemical signal of TBO in the amperometric method (Scheme 1). The stock solution of thrombin (100 μM) was prepared in 0.1 M PBS saline (pH 7.4) and was then diluted to appropriate concentrations for a calibration curve. The MNP@Ab-TBO solution was incubated to various concentrations of thrombin solution with the volume ratio of 1:1 for 4 min.

The quantitative analysis of thrombin in PBS saline and human serum sample was based on the reduction current of TBO by the MNP@Ab-TBO captured on the pTBA/Apt/thrombin. The measured currents (ΔI) for various thrombin concentrations were obtained from the baseline signal at 10 s. The reliability of the amperometric aptasensor was evaluated through the determination of the thrombin in human serum samples (10, 100, 200, and 500 nM) as shown in Fig. 5. The analysis of thrombin was performed three times for each sample. The current response was proportionally increased to the thrombin concentration (inset of Fig. 5). The linear regression equation of the calibration plot showed the ΔI_P (nA) = 0.967 (± 0.011) + 0.190 (± 0.009) [thrombin] (nM) with correlation coefficient of 0.984. The proposed sensor was validated with thrombin-spiked human serum samples, and the recovery of the spiked sample was in the range 93.8 ~ 103.6% (Table S2). The recoveries indicate that the accuracy of the proposed sensor with high sensitivity and selectivity for detecting thrombin in serum samples.

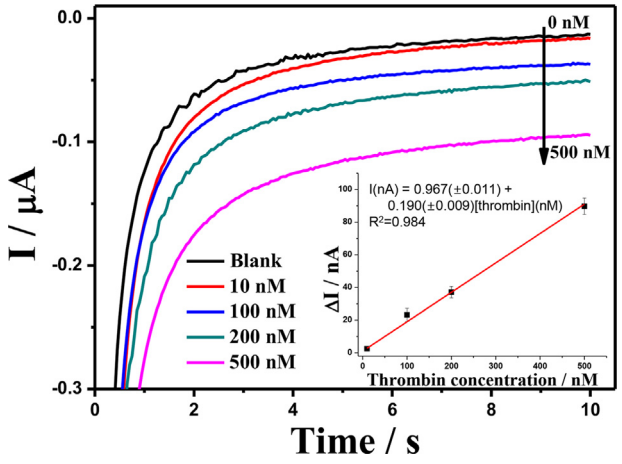

Fig. 5. Quantitative detection of thrombin in serum samples using magnetic force-assisted electrochemical sandwich assays (inset: calibration plot for various concentrations of thrombin).

4. Conclusion

A magnetic force assisted electrochemical aptamer-antibody sandwich assay (MESA) has been successfully developed to simplify the detection step without washing by controlling a magnetic field. The proposed sensor could detect the thrombin in human serum within 7 min, which is simple, easy-to-use, stable, and fast response time compared to the previous reports. However, the proposed method requires an electro-magnet, additionally. A linear relationship for thrombin detection was observed between 1 and 500 nM, with the detection limit of 0.49 (± 0.06) nM (RSD < 4.3%), which is appropriate for the clinical application. Therefore, the developed method can be used as a point-of-care device, which has sought a method for simple, automated, and accurate detection of other disease markers from a drop of biological fluids in a hand-held device type.

Acknowledgements

This work was supported by the researcher program from National Research Foundation of Korea (NRF) grant funded by the Korea government (MSIP) (No. 2015R1A2A1A13027762). J. C. and H. H. thank to the Ministry of Trade, Industry and Energy (MOTIE, Korea) for support of the research (No. 10067197).

Conflict of interest

The authors declare that there are no conflicts of interest.

Appendix A. Supplementary material

Supplementary data associated with this article can be found in the online version at http://dx.doi.org/10.1016/j.bios.2018.06.068.

References

Centi, S., Tombelli, S., Minunni, M., Mascini, M., 2007. Anal. Chem. 79, 1466–1473.
Chandra, P., Koh, W.C.A., Noh, H.-B., Shim, Y.-B., 2012. Biosens. Bioelectron. 32, 278–282.
Chin, C.D., Laksanasopin, T., Cheung, Y.K., Steinmiller, D., Linder, V., Parsa, H., Wang, J., Moore, H., Roouse, R., Umviligihozo, G., Karita, E., Mwambarangwe, L., Braunstein, S.L., van de Wijgert, J., Sahabo, R., Justman, J.E., El-Sadr, W., Sia, S.K., 2011. Nat. Med. 17, 1015–1019.
Coughlin, R.S., 2000. Nature 407, 258–264.
Eguílaz, M., Moreno-Guzmán, M., Campuzano, S., González-Cortés, A., Yá˜nez-Sede˜no, P., Pingarrón, J.M., 2010. Biosens. Bioelectron. 26, 517–522.
Fan, R., Vermesh, O., Srivastava, A., Yen, B.K.H., Qin, L., Ahmad, H., Kwong, G.A., Liu, C.-C., Gould, J., Hood, L., Heath, J.R., 2008. Nat. Biotechnol. 26, 1373–1378.
Gao, F., Du, L., Tang, D., Lu, Y., Zhang, Y., Zhang, L., 2015a. Biosens. Bioelectron. 66, 423–430.
Gao, F., Qian, Y., Zhang, L., Dai, S., Lan, Y., Zhang, Y., Du, L., Tang, D., 2015b. Biosens. Bioelectron. 71, 158–163.
Gao, F., Du, L., Zhang, Y., Zhou, F., Tang, D., 2016. Biosens. Bioelectron. 86, 185–193.
Gong, P., Li, H., He, X., Wang, K., Hu, J., Tan, W., Zhang, S., Yang, X., 2007. Nanotechnology 18, 285604.
Green, N.M., 1970. Method. Enzymol. 18, 418–424.
Han, Q., Shen, X., Zhu, W., Zhu, C., Zhou, X., Jiang, H., 2016. Biosens. Bioelectron. 79, 180–186.
He, P., Shen, Li, Cao, Y., Li, D., 2007. Anal. Chem. 79, 8024–8029.
Hwang, H., Chon, H., Choo, J., Park, J.-K., 2010. Anal. Chem. 82, 7603–7610.
Inuyama, H., Saito, T., Takagi, J., Saito, Y., 1997. J. Cell. Physiol. 173, 406–414.
Iqbal, S.S., Mayo, M.W., Bruno, J.G., Bronk, B.V., Batt, C.A., Chambers, J.P., 2000. Biosens. Bioelectron. 15, 549–578.
Jebaramya, J., Ilanchelian, M., Sprabahar, S., 2009. Dig. J. Nanomater. Biostruct. 4, 789–797.
Kim, D.-M., Yoon, J.H., Won, M.S., Shim, Y.B., 2012. Electrochim. Acta 67, 201–207.
Koh, W.C.A., Chandra, P., Kim, D.-M., Shim, Y.-B., 2011. Anal. Chem. 83, 6177–6183.
Luddington, R., Baglin, T., 2004. J. Thromb. Haemost. 2, 1954–1959.
Macfarlane, R.G., Biggs, R.A., 1953. J. Clin. Pathol. 6, 3–8.
Min, K., Song, K.M., Cho, M., Chun, Y., S., Shim, Y.-B., Ku, J.K., Ban, C., 2010. Chem. Commun. 46, 5566–5568.
Mir, M., Vreeke, M., Katakis, I., 2006. Electrochem. Commun. 8, 505–511.
Moon, J.-M., Kim, D.-M., Kim, M.H., Han, J.-Y., Jung, D.-K., Shim, Y.-B., 2017. Biosens. Bioelectron. 91, 128–135.
Moon, J.-M., Thapliyal, N., Hussain, K.K., Goyal, R.N., Shim, Y.-B., 2018. Biosens. Bioelectron. 102, 540–552.
Naveen, M.H., Gurudatt, N.G., Shim, Y.-B., 2017. Appl. Mater. Today 9, 419–430.
Nierodzik, M.L., Karpatkin, S., 2006. Cancer Cell 10, 355–362.
Polsky, R., Gill, R., Kaganovsky, L., Willner, I., 2006. Anal. Chem. 78, 2268–2271.
Qian, Y., Gao, F., Du, L., Zhang, Y., Tang, D., Yang, D., 2015. Biosens. Bioelectron. 74, 483–490.
Rand, M.D., Lock, J.B., van't Veer, C., Gaffney, D.P., Mann, K.G., 1996. Blood 88, 3432–3445.
Shuman, M.A., Majerus, P.W., 1976. J. Clin. Invest. 58, 1249–1258.
Srinivas, R.L., Chapin, S.C., Doyle, P.S., 2011. Anal. Chem. 83, 9138–9145.
Tan, W.H., Wang, K.M., Drake, T.J., 2004. Curr. Opin. Chem. Biol. 8, 547–553.
Tasset, D.M., Kubik, M.F., Steiner, W., 1997. J. Mol. Biol. 272, 688–698.
Tennico, Y.H., Hutanu, D., Koesdjojo, M.T., Bartel, C.M., Remcho, V.T., 2010. Anal. Chem. 82, 5591–5597.
Wang, C., Qian, Y., Zhang, Y., Meng, S., Wang, S., Li, W., Gao, F., 2017. Sens. Actuators B-Chem. 238, 434–440.
Willner, I., Zayats, M., 2007. Angew. Chem. Int. Ed. Engl. 46, 6408–6418.
Zhu, Y., Chandra, P., Shim, Y.-B., 2013. Anal. Chem. 85, 1058–1064.